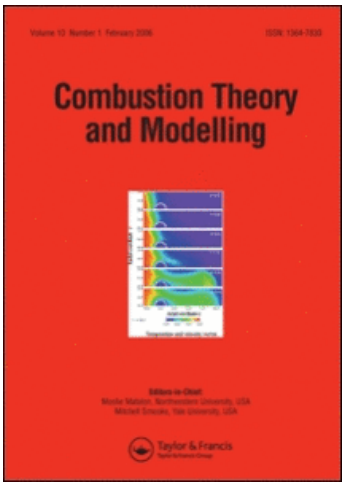

Combustion Theory and Modelling
Publication details, including instructions for authors and subscription information:
http://www.informaworld.com/smpp/title~content=t713665226

Effects of compression and stretch on the determination of laminar flame speeds using propagating spherical flames

Z. Chen [a]; M. P. Burke [a]; Y. Ju [a]
[a] Department of Mechanical and Aerospace Engineering, Princeton University, Princeton, NJ, USA

Online Publication Date: 01 April 2009

To cite this Article Chen, Z., Burke, M. P. and Ju, Y.(2009)'Effects of compression and stretch on the determination of laminar flame speeds using propagating spherical flames',Combustion Theory and Modelling,13:2,343 — 364
To link to this Article: DOI: 10.1080/13647830802632192
URL: http://dx.doi.org/10.1080/13647830802632192

Combustion Theory and Modelling
Vol. 13, No. 2, 2009, 343–364

Taylor & Francis
Taylor & Francis Group

Effects of compression and stretch on the determination of laminar flame speeds using propagating spherical flames

Z. Chen*, M. P. Burke and Y. Ju

Department of Mechanical and Aerospace Engineering, Princeton University, Princeton, NJ 08544, USA

(*Received 17 January 2008; final version received 1 November 2008*)

The effects of flow compression and flame stretch on the accurate determination of laminar flame speeds at normal and elevated pressures using propagating spherical flames at constant pressure or constant volume are studied theoretically and numerically. The results show that both the compression-induced flow motion and flame stretch have significant impacts on the accuracy of flame speed determination. For the constant pressure method, a new method to obtain a compression-corrected flame speed (CCFS) for nearly constant pressure spherical bomb experiments is presented. Likewise, for the constant volume method, a technique to obtain a stretch-corrected flame speed (SCFS) at elevated pressures and temperatures is developed. The validity of theoretical results for both constant pressure and constant volume methods is demonstrated by numerical simulations using detailed chemistry for hydrogen/air, methane/air, and propane/air mixtures. It is shown that the present CCFS and SCFS methods not only improve the accuracy of the flame speed measurements significantly but also extend the parameter range of experimental conditions. The results can be used directly in experimental measurements of laminar flame speeds.

Keywords: laminar flame speed; spherical flame; compression effect; flame stretch rate

1. Introduction

The laminar flame speed is defined as the speed relative to the unburned gas, with which a planar, one-dimensional flame front travels along the normal to its surface [1]. It is one of the most important parameters of a combustible mixture. On a practical level, it affects the fuel burning rate in internal combustion (IC) engines and the engine's performance and emissions [2]. On a more fundamental level, it is an important target for the validation of kinetic mechanisms [3]. *Accurate* determination of flame speeds at high pressures and temperatures is extremely important for the development and validation of kinetic mechanisms for gasoline and diesel surrogate fuels and alternative fuels [3–5].

In the last 50 years, substantial attention has been given to the development of new techniques and the improvement of existing methodologies for experimental and theoretical determination of the laminar flame speed. Various experimental approaches, reviewed in [1, 6], have been developed to measure the flame speed utilising different flame configurations, including the outwardly propagating spherical flame [2, 4, 6–23], counterflow or stagnation flame [24–27], Bunsen flame [17], and burner stabilised flat flame [28, 29].

*Corresponding author. Currently at Peking University. Email: chenzheng@coe.pku.edu.cn

ISSN: 1364-7830 print / 1741-3559 online

DOI: 10.1080/13647830802632192
http://www.tandf.co.uk/journals

Owing to the lack of uniformity of the flame speed over the flame surface in the Bunsen flame and the wall effects in the flat flame, the propagating spherical flame and the stationary counterflow flame are among the most successful systems for flame speed measurements [6, 10]. However, owing to the Reynolds number limit, the counterflow flame method is difficult to apply at high pressures (e.g. above 10 atm) [10]. Consequently, tracking the evolution of an outwardly propagating spherical flame in a confined bomb is the most favorable method for measuring the flame speed, especially at pressure above 10 atmosphere [2, 4, 10, 13].

Historically, spherical bombs for laminar flame speed measurements have been very large, limiting them of course to low pressure (below 10 atmosphere) study. For one of the two common spherical flame methods (both of which are described below), the constant pressure method, they are large so that pressure rise in the chamber is not significant during the portion of the flame propagation of interest; for the constant volume method, they are large so that curvature and stretch effects can be neglected. However, there are several important merits to smaller combustion bombs. First of all, for both constant pressure and volume methods, a smaller chamber allows for higher pressure measurements while maintaining the same level of operational safety. Second, a smaller chamber requires less material to construct and so it is cheaper than a larger one. It is much easier to prepare homogeneous pre-mixture in a smaller chamber, especially for gaseous large hydrocarbon fuels vaporised from liquid phase, and to heat up a smaller chamber for experiments measuring laminar flame speed at high temperature. Finally, a smaller chamber used for the constant volume method can actually allow measurements that would be impossible using a larger chamber. For example, the effects of radiation and hydrodynamic instabilities become more important at large flame radii. In smaller combustion chambers, these effects would be minimised during the portion of the propagation that produces pressure rises large enough to be detected by the pressure transducer. The theoretical models developed in this study account for the effects of compression and stretch, which have previously set lower limits on the size of spherical explosion bombs. As such, proposed methods enable the use of smaller chambers allowing all of the methods described above.

In the propagating spherical flame method, a quiescent homogeneous combustible mixture in a closed chamber is centrally ignited by an electrical spark or a laser beam which results in an outwardly propagating spherical flame [6, 17]. The flame front history and/or the pressure rise history are/is recorded during the experiment and related to the laminar flame speed through theoretical models [6, 17] which are described in the next section. Depending on the bomb design and the pressure change, there are two different methods for flame speed measurement by using the expanding spherical flames. The so-called constant pressure method [4, 5, 8–16] uses Schlieren or shadow photograph to view the flame front propagation history of an expanding spherical flame in a large confined chamber or a pressure release dual-chamber. There are two main advantages of this method. First, the propagating flame surface is observed such that any cellular instability that might develop over the flame surface during its propagation can be revealed. Second, since the effect of pressure and temperature rise on flame speed is minimal during the early stages, there exists a stage where the flame speed is purely a function of stretch, allowing for extrapolation to zero stretch and determination of stretch behaviour. Recently a great deal of effort has been devoted to obtaining accurate flame speeds utilising this method. For example, Burke *et al*. [30] demonstrated that the effect of flow field deviation due to constant-pressure nonspherical chambers can significantly affect the accuracy of flame speed measurements; Chen *et al*. [31] found that the incoming flow induced by the radiative cooling of the high temperature products inside a spherical flame will slow the flame propagation, thus greatly

decreasing the accuracy of flame speed measurements for highly radiative mixtures; Kelley and Law [32] suggested that nonlinear extrapolation between stretched flame speed and stretch rate should be used for mixtures with Lewis numbers appreciably different from unity; Chen *et al*. [33] showed that the ignition energy has a significant impact on the flame trajectories and that the flame speed reverse phenomenon owing to unsteady flame transition greatly narrows the experimental data range that is valid for flame speed extrapolation. All the models on the constant pressure method utilised in previous studies are based on the assumption of zero burned gas velocity. However, the validity of this assumption has not been confirmed, particularly when small combustion chambers are used to achieve higher pressures while ensuring operational safety.

The other experimental technique, the so-called constant volume method [2, 5, 17–23] employs a fast-response pressure transducer to measure the chamber pressure history during the propagation of an expanding spherical flame in a closed thick-walled spherical vessel. Conversion of the reactants to hot products across the flame front results in a rapid pressure rise and a corresponding temperature rise in unburned and burned gas. Therefore, this method has the advantage that the flame speed for a given mixture over a wide range of temperatures and pressures can be obtained from a single test [2]. The spherical constant-volume vessel technique for determining laminar flame speed was initially developed and utilised in [17–19]. Recently, several improved theoretical models to relate the experimentally measured pressure history to the instantaneous flame speeds have been developed. Saeed and Stone [20] developed a multiple burned gas zone model to allow for a more realistic temperature distribution within the burned gas than the initially employed uniform temperature assumption. Metghalchi and coworkers [22] considered a variable-temperature central burned gas core surrounded by a preheat zone, an uniform-temperature unburned gas shell, and a thermal boundary layer at the wall in their model, and they accounted for different sources of heat loss. Huzayyin *et al*. [23] revealed that using different models to relate the pressure history to the same flame speed for the same experimental data results in discrepancies of up to 15% in the calculated flame speed. The result indicates the importance of accurate models and the need to improve them further. In all of the models, it is assumed that the stretch effect on flame speed is negligible. However, in practical measurements for hydrogen and high-molecular-weight hydrocarbon fuels, the effect of flame stretch for the experimental conditions is not always of a negligible magnitude [25]. Therefore, the inclusion of flame stretch is necessary for a more comprehensive and more accurate model.

It is also found that discrepancies exist among flame speed data obtained from measurements of spherical flames and counterflow flames [5]. The reason for this discrepancy has yet to be qualitatively explained. One possible source is the interpretation of the experimental data, particularly for data at conditions lie outside of the parameter range over which the assumptions in the models are justified. Although both constant pressure and constant volume methods are popularly utilised in measuring flame speed in a broad range of pressures, due to the complexity of flame stretch, flow compression, flame structure, chamber geometry, and thermal radiation, the accuracy and the validity of the employed models for flame speed measurement over a certain parameter range in both methods still remain unclear. For example, in the constant pressure method, the stretched flame speed is first obtained from the flame front history, $R_f = R_f(t)$, and then is linearly extrapolated to zero stretch rate to obtain the unstretched flame speed. Flame speeds are commonly extrapolated over ranges of flame radius data, $[R_{fL}, R_{fU}]$ [4, 5, 8–16]. The lower bound, R_{fL}, is often chosen to reduce the effects of initial spark ignition, flame curvature, and unsteadiness on the flame propagating speed, and to make stretch rate small such that the linear relationship between stretched flame speed and stretch rate is satisfied [33, 34]. The upper bound, R_{fU}, is frequently chosen to ensure that the pressure change is 'small'

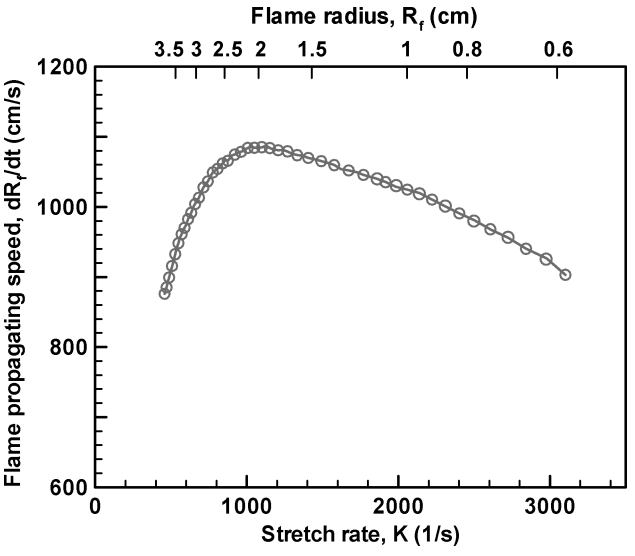

Figure 1. Experimental results on flame propagating speed of H_2/air flame ($\varphi = 3$) as functions of stretch rate and flame radius.

[4, 5, 8–16]. Historically, the choice of data range has been somewhat arbitrary: different researchers made different choices without giving quantitative justification. The range should be large enough to ensure accurate extrapolation, since the uncertainty in the extrapolation decreases with the increase of stretch rate range.

Figure 1 shows the flame propagating speed as a function of stretch rate or flame radius for hydrogen/air (equivalence ratio $\varphi = 3.0$) propagating spherical flames from experiments in a constant-pressure cylinder chamber (the details on experimental setup and procedures could be found in references [4, 15, 30]). It is apparent that different unstretched flame speeds would be obtained from linear extrapolation of the experimental data based on different flame radii ranges. To the authors' knowledge, there is no quantitative study on how the flame radii range, $[R_{fL}, R_{fU}]$, affects the measured flame speed and how to choose the proper R_{fU} in the literature. Moreover, in all the previous studies [4, 5, 8–16], the choices of the R_{fU} were solely based on the pressure dependence of the flame speed. However, the effect of nonzero burned gas velocity generated by pressure wave compression, which renders the assumption of 'zero burned gas velocity' invalid, has not been discussed. Figure 1 shows that the propagating speed measured from experiments will decrease when the flame radius is larger that 2.2 cm owing to the nonzero burned gas velocity which slows down the flame propagation. As will be shown in this study, this compression-induced nonzero burned gas velocity can significantly affect the accuracy of the measured flame speed. This paper focuses on the compression effect for the constant pressure method in spherical chambers addressing two main concerns. First, how much does flow compression affect the accuracy of flame speed measurement for a small pressure increase? Second, how does one correct for the compression effect in the flame speed measurements? Since the pressure increase during flame propagation depends cubically on the ratio of flame radius, R_f, and chamber size, R_0, smaller upper, R_{fU}, should be specified for a smaller chamber and thus the flame radii range, $[R_{fL}, R_{fU}]$, might be too narrow for data processing. In this case, correction for the compression effect allows for a wider range that can be used for extrapolation, resulting in a more accurate unstretched flame speed.

Similarly, in the constant volume method, the stretch effect on the laminar flame speed might be too large to be neglected for mixtures with Lewis numbers greatly deviating from unity and thus the stretch correction for obtaining accurate unstretched laminar flame speed is indispensable [25]. As shown in Figure 1, when the flame size is small, the stretch rate is more than 1000 s^{-1}. For rich hydrogen/air flame of equivalence ratio 3.0, the burned Markstein length is about 0.08 cm, thus decrease of flame propagating speed caused by stretch effect is more than 80 cm/s. However, in all previous studies [2, 19–23], the effect of flame stretch was neglected. Similarly for the stretch effect as the compression effect, this paper focuses on the stretch effect for the constant volume method addressing two concerns. First, how much does the stretch affect the accuracy of flame speed measurement? Second, how does one correct for the stretch effect in the flame speed measurements?

The objective of the present study is to answer the questions posed above. For the constant pressure method, the effects of flow compression and different flame radii ranges on the accuracy of flame speed measurements will be investigated, and by including the compression effect, the compression-corrected flame speed (CCFS) will be presented. For the constant volume method, the stretch effect on the measured flame speed will be studied and a method to obtain a stretch-corrected flame speed (SCFS) at elevated pressures and temperatures will be presented. For both methods, the validity of theoretical models and the improvement in the accuracy of measured flame speed will be demonstrated by numerical simulations of hydrogen/air, methane/air, and propane/air flames using detailed chemistry. In this study, detailed numerical simulations instead of experimental measurement have been utilised because: 1), the compression induced flow field (which is difficult to measure in experiments) could be readily obtained from simulation and thus be compared with theoretical model; and 2), other effects such as radiative loss (which always exist in experiments) could be excluded in simulation in order to isolate the effects of interest in this study.

The paper is organised as follows: in section 2, theoretical models of flame speed measurement are introduced, and the CCFS and SCFS are presented for the constant pressure and constant volume methods, respectively. Then, in section 3 the validity of theoretical models and the improvement in the accuracy of measured flame speed are demonstrated by numerical simulations using detailed chemistry. Finally, the conclusions are given in section 4.

2. Theoretical models of flame speed measurement

The theoretical models of flame speed measurements utilising the constant pressure and constant volume methods are briefly presented in the following two subsections. The compression and stretch effects are studied analytically, and the CCFS and SCFS are proposed.

2.1. *The constant pressure method and the compression effect on flame speed*

In the constant pressure method (the details of this method could be found in Refs. [8, 11, 16, 34]), the flame speed is obtained from the flame front history, $R_f = R_f(t)$, recorded by using the Schlieren or shadow photograph. There are different methods found in the literature for relating the stretch rate and the stretched flame speeds such that the unstretched laminar flame speed and Markstein length can be extracted as described in [4, 5, 8–16]. In the present study, we will use the definition of Clavin [35]

$$S_u = S_u^0 - L_u K \tag{1}$$

where S_u^0 and S_u are respectively the unstretched and stretched flame speed with respect to the unburned mixture, L_u the unburned Markstein Length, and K the flame stretch rate. For outwardly propagating spherical flames, the flame stretch rate is $K = 2R_f^{-1}(dR_f/dt)$. According to the kinetic balance with respect to the burned mixture and mass conservation, the stretched flame speed is give by [36]

$$S_u = a\frac{dR_f}{dt} - aU_b \tag{2}$$

where $a = \rho_b/\rho_u$ is the density ratio between the burned and unburned mixtures and U_b the flow velocity of burned gas behind the flame front (positive in the outward direction). In all the previous studies utilising the constant pressure method [4, 5, 8–16], data reduction was performed only for 'small' pressure change and the burned gas is assumed to be quiescent ($U_b \approx 0$). As a result, the moving velocity of the experimentally visualised flame front is the burned flame speed

$$S_u \approx a(dR_f/dt) \tag{3}$$

Therefore, according to Equation (1), the unstretched laminar flame speed, S_u^0, and Markstein Length, L_u, can be obtained from the linear extrapolation based on the plot of $S_u - K$, where S_u and K are both calculated from flame front history $R_f = R_f(t)$.

However, as will be shown in section 3, neglecting the compression-induced flow velocity U_b even at a small pressure increase might significantly decrease the accuracy of the measured flame speed. By considering pressure increase, the following relationship is found for expanding flames in a closed spherical chamber [17–19]

$$S_u = a\frac{dR_f}{dt} + a\frac{R_f}{3\gamma P}\frac{dP}{dt} \tag{4}$$

where γ is the ratio of heat capacities, and P is the pressure which is nearly uniform in the closed chamber [17]. By comparing Equations (2) and (4), the flow velocity of the burned gas behind the flame front is

$$U_b = -\frac{R_f}{3\gamma P}\frac{dP}{dt} \tag{5}$$

The pressure and its rate of change in Equation (5) can be either measured directly in experiments or calculated from the flame front history by the Schlieren images [18]

$$\frac{R_f}{R_0} = \left[1 - \frac{P_e - P}{P_e - P_0}\left(\frac{P_0}{P}\right)^{1/\gamma}\right]^{1/3} \tag{6}$$

where P_0 and P_e are the initial and final chamber pressures, respectively, and R_0 is the radius of a spherical chamber (which is the equivalent radius, $R_0 = (3V/4\pi)^{1/3}$, for a nonspherical chamber of volume V).

With the increase of the pressure, the unburned gas temperature, T_u, will also increase so that the density ratio, a, is not a constant but a function of T_u

$$a(T_u) = T_u/T_{ad} = (1 + \Delta T/T_u)^{-1} \tag{7}$$

where ΔT is the temperature increase caused by chemical heat release and it can be calculated from thermodynamic quantities. Assuming the unburned gas is compressed isentropically, T_u can be calculated from the pressure, which could be obtained from the flame front history according to Equation (6), $T_u = T_0(P/P_0)^{(1-1/\gamma)}$. Then T_u and thus $a = a(T_u)$ can also be calculated from the flame front history. Note that when the flame radius is less than half of chamber radius, the change of the flame speed due to pressure and temperature increase alone is less than 1% which is negligible compared to the changed caused by compression-induced flow.

Therefore, the compression-induced flow velocity, U_b, can be evaluated from the flame front history by using Equations (5) and (6). As a result, flame speed extrapolated by using Equation (2) instead of (3) is more accurate due to the inclusion of the compression effect. The unstretched flame speed, S_u^0, obtained by linear extrapolation of S_u given by Equations (2), (5) and (6), is called the compression-corrected flame speed (CCFS). As will be shown in section 3, the accuracy of the measured flame speed is greatly improved by using CCFS.

2.2. *The constant volume method and the stretch effect on flame speed*

The constant volume method also uses a spherical vessel with central ignition. However, it calculates the flame speed based on the pressure history $P = P(t)$ recorded after the flame has grown to a sufficiently large size such that the pressure variation is evident. The details of theoretical analysis on this method can be found in references [2, 17–19, 21]. Based on the following assumptions: the flame is thin, smooth, and spherical; the pressure is spatially uniform; the constituents of the burned and unburned gases behave as ideal gases; the dissociation products are in equilibrium; the unburned gas is compressed isentropically; and buoyancy effects are negligible, the following expressions for flame speed, S_u, could be obtained [17–19]

$$S_u = \frac{R_0^3}{3R_f^2}\left(\frac{P_0}{P}\right)^{1/\gamma}\frac{dx}{dt} \tag{8}$$

$$\frac{R_f}{R_0} = \left[1 - (1-x)\left(\frac{P_0}{P}\right)^{1/\gamma}\right]^{1/3} \tag{9}$$

where x is the ratio between the burned and total masses. For simplicity, the commonly employed assumption of a linear relationship between mass fraction of burned gas and pressure rise is employed [17–19]

$$x = \frac{P - P_0}{P_e - P_0} \tag{10}$$

The validity of this assumption is confirmed by detailed numerical simulation in section 3 (Figure 7). Substituting Equation (10) into (8) and (9), the relationship in Equation (6) is

readily obtained and the flame speed is given by

$$S_u = \frac{R_0}{3}\left(\frac{R_0}{R_f}\right)^2 \frac{1}{(P_e - P_0)}\left(\frac{P_0}{P}\right)^{1/\gamma_u}\frac{dP}{dt} \tag{11}$$

Therefore, from the pressure history $P = P(t)$, the flame position R_f could be obtained according to Equation (6) and the stretched flame speed S_u could be evaluated by using Equation (11).

In all previous experimental studies [2, 5, 17–23], the flame speed, S_u, obtained from the constant volume method is actually the stretched flame speed, not the unstretched flame speed, S_u^0. As mentioned before, the stretch effect on flame speed might be significant for mixtures with Lewis numbers greatly deviating from unity (see Figure 1). In the present section, the effects of flame stretch on the measured flame speed will be analysed, and a method that includes a stretch correction in the determination of flame speed measurements will be introduced.

The stretch effect on flame speed is given by Equation (1). Note that to zeroth order, we have $S_u \approx S_u^0$. So Equation (1) can be written as

$$\frac{S_u^0 - S_u}{S_u^0} \approx \frac{L_u K}{S_u} \tag{12}$$

With the definition of stretch rate and the flame radius in term of pressure given by Equation (6), the following expression for flame stretch rate can be derived

$$K = \frac{2}{3}\left(\frac{R_0}{R_f}\right)^3 \left(1 + \frac{P_e - P}{\gamma P}\right)\frac{1}{P_e - P_0}\left(\frac{P_0}{P}\right)^{1/\gamma}\frac{dP}{dt} \tag{13}$$

By using Equations (6), (11–13), the relative difference of flame speed caused by the stretch effect can be obtained as

$$\frac{S_u^0 - S_u}{S_u^0} \approx \frac{2L_u}{R_f}\left(\frac{\gamma - 1}{\gamma} + \frac{P_e}{\gamma P}\right) \tag{14}$$

According to the above equation, the error in the measured flame speed caused by neglecting the stretch effect can be evaluated. It is apparent from Equation (14) seen that the error is proportional to the Markstein length and the inverse of flame radius. Furthermore, when the flame size is small, the pressure increase is small and thus P_e/P is large, so the stretch effect is further magnified by the term inside the brackets in Equation (14). Therefore, for small spherical flames in mixtures with Lewis numbers greatly deviating from unity, the stretch effect on the flame speed is significant so a stretch correction is necessary. Figure 2 shows the error caused by neglecting the stretch effect according to Equation (14) for a typical run with $P_e/P_0 = 8.27$, $\gamma = 1.4$, $L_u = 0.3$ mm (close to the Markstein length of rich hydrogen/air and lean propane/air flames, as will be shown in section 3) and chamber size $R_0 = 6$ cm. It is observed that the stretch effect on flame speed is greater than 10% when the pressure increase is below 20% ($P/P_0 < 1.2$ or $R_f/R_0 < 0.54$). Therefore, the stretch correction is necessary for accurate determination of the

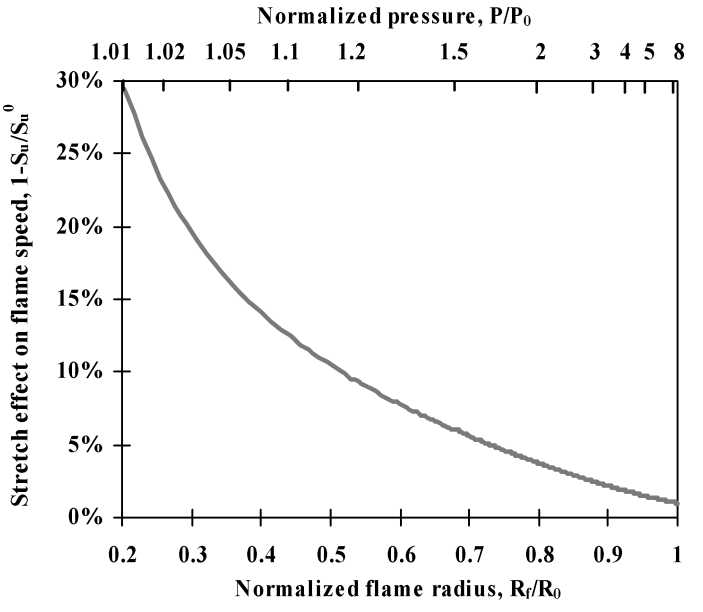

Figure 2. The stretch effect on the flame speed according to Equation (14) with $P_e/P_0 = 8.27$, $\gamma = 1.4$, $L_u = 0.3$ mm, $R_0 = 6$ cm.

laminar flame speed. Note that the ratio of specific heats, γ, is assumed to be constant (γ=1.4) in SCFS. Numerical simulations show that the change of γ (less than 3%) with the temperature, pressure and composition during the flame propagation is negligible.

In order to obtain a more accurate flame speed, stretch-corrected flame speed (SCFS), S_u^0, is proposed here. The SCFS is obtained by applying a stretch correction according to Equation (1), in which the stretched flame speed, S_u, is calculated from the measured pressure history according to Equations (11) and (6), and the stretch rate, K, is calculated according to Equation (13). Note that in Equation (1), the calculation of SCFS requires a value for the Markstein length, L_u. The Markstein length, which is usually measured either from propagating spherical flames using the constant pressure method discussed in above [11–16] or from counterflow flame experiments [26, 27], can be obtained from linear extrapolation of stretched flame speed, S_u, and flame stretch rate, K, calculated from the pressure history (according to Equations (6), (11), and (13)) over spans of data where the pressure and temperature increase is small for the constant volume method. Since the temperature and pressure of the unburned gas will increase during the flame propagation, the flame speed is affected not only by the stretch rate but also by the increases of the temperature and pressure of the unburned gas. This was also shown by theoretical analysis by Sivashinshky [37, 38] and Bechtold and Matalon [39]. Therefore, the Markstein length can not be obtained accurately from the linear extrapolation of S_u and K calculated from pressure history when the pressure increase is large (above 5%) for the constant volume method. However, there exists a portion of the flame propagation where the pressure rise is detectable experimentally, but the flame speed is nearly insensible to the changes in temperature and pressure and is almost purely a function of stretch rate. As will be shown by the numerical simulations in the next section, the Markstein length corresponding to mixtures at the initial pressure can be accurately obtained from the pressure history during this period and can be utilised in the SCFS method to improve the accuracy of the flame speed measurement.

3. Numerical validation of models

In this section, the validity of the theoretical results presented in section 2 is demonstrated by numerical simulations of outwardly propagating spherical flames of hydrogen/air, methane/air, and propane/air mixtures in a closed spherical chamber using detailed chemistry. Specifically, the flow compression and flame stretch effects will be studied, and the improvement in the accuracy of flame speed determination using the CCFS and SCFS methods will be shown for the constant pressure and volume methods, respectively.

A time-accurate and space-adaptive numerical algorithm for the Adaptive Simulation of Unsteady Reacting Flow, A-SURF (1D), has been developed to carry out high-fidelity numerical simulations of the outwardly propagating spherical flame in a closed chamber under a broad range of pressures. A-SURF (1D) has been successfully used in our previous studies of radiation absorption effect and ignition effect on outwardly propagating spherical flames [33, 40]. The details on the governing equations and numerical methods of A-SURF are presented in the supplemental materials of Ref. [33]. For the propagating spherical flame in a closed chamber, due to the pressure change and the pressure induced compression wave, the unsteady compressible Navier-Stokes Equations for multi-component reactive flow are solved. The finite volume method is employed for discretising the conservation governing equations in the spherical coordinate. The second-order-accurate Strang splitting fractional-step procedure [41] is utilised to separate the time evolution of the stiff reaction term from that of the convection and diffusion terms. In the first fractional step, the nonreactive flow is solved. The Runge–Kutta, central difference, and MUSCL-Hancock [42] schemes, all of second-order accuracy, are employed for the calculation of the temporal integration, diffusive flux, and convective flux, respectively. The chemistry is solved in the second fractional step by using the VODE solver [43]. Detailed chemistry is included in the simulation and the thermodynamic and transport properties are evaluated using the CHEMKIN and TRANSPORT packages [44, 45].

The reaction zone is usually very thin and the flame thickness is strongly affected by pressure. In order to maintain adequate numerical resolution of the moving flame front without the need to use hundreds of thousands of grid points, a multi-level, dynamically adaptive mesh refinement algorithm has been developed. Local mesh addition and removal are based on the first- and second-order gradients of the temperature, velocity and major species distributions. Seven to ten grid levels are utilised in this study and the moving reaction zone is always fully covered by the finest meshes of 32 μm to 4 μm in width. Simulations using smaller finest meshes have also been conducted and confirmed the adequacy of the above grid size for achieving accurate solutions.

Moreover, the unstretched laminar flame speed of the adiabatic planar flame, S_L, is calculated using the steady one-dimensional laminar premixed flame code, PREMIX, due to Kee *et al*. [44]. It is found that the maximum relative differences between the adiabatic planar (unstretched) flame speed obtained from PREMIX and A-SURF over the entire test range is less than 2% (the mixture-averaged diffusion including thermal diffusion is utilised in both PREMIX and A-SURF), which demonstrates the robustness and accuracy of the present computation methods [33]. Therefore, A-SURF can accurately model outwardly propagating spherical flames and thus can be employed to validate the theoretical models for flame speed measurements utilising expanding flames.

In all the simulations, the spherical chamber radius is set to be $R_0 = 6$ cm. All the results in the following parts are presented in terms of flame radii normalised by the chamber size (R_f/R_0). Therefore, the same conclusions still hold for the cases using other chamber sizes (normalised results from simulations with $R_0 = 12$ cm show qualitatively similar results as

those with $R_0 = 6$ cm). The flame is initiated by a small hot pocket ($\sim$1 mm in radius) of burned products surrounded by fresh mixture at the room temperature and pressure ($T_0 = 298\ K$, $P_0 = 1$ atm). At the inner and outer boundaries at $r = 0$ and $r = R_0$, respectively, zero-gradient conditions are enforced. The size of the hot pocket is small enough and it does not affect the flame speed because for both methods, only the data for flame radii larger that 6 mm are utilised to calculate the flame speed in this study. The current simulations as well as those by Bradley *et al*. [34] have confirmed that the ignition effect on flame speed is negligible once the flame radius is larger than 6 mm for the conditions studied. In order to focus on the compression and stretch effects, the effects of radiation (for most mixtures such as H_2/air, CH_4/air, and C_3H_8/air not close to flammability limits and without CO_2 dilution, the radiation effect could be neglected) [8, 40, 46], buoyancy, and heat loss to the chamber wall [22] on flame speed are not considered here.

To validate the robustness of the theoretical models, simulations utilising detailed chemistry for different fuels (H_2, CH_4 and C_3H_8) have been carried out and will be shown in the following two subsections. To simulate the H_2/air flames, the recent mechanism of 9 species and 25 reactions developed by Li *et al*. [47] is employed. For CH_4/air, the GRI-MECH 3.0 mechanism [48] is used. To save computation time, the NOx sub-mechanism is not included and the resulting mechanism contains 36 species and 219 reactions. For C_3H_8/air, San Diego Mechanism 20050615 [49] which consists of 40 species and 175 reactions is utilised.

3.1. *Results for the constant pressure method*

For the constant pressure method, similar to the Schlieren imaging in the experiments, the flame front history, $R_f = R_f(t)$, from the numerical simulation is used to calculate the flame speed. In the simulation, the position of flame front is defined as the position of maximum heat release (It was pointed out that the level of contours chosen to track the flame front might affect the flame front propagating speed [34]. However, this second-order effect is important only for very lean or rich pre-mixtures which have much thicker reaction zones [8]). The chamber pressure can be either obtained from simulation or calculated from flame front history by solving Equation (6). The difference between the pressures obtained from those two methods is negligible. The compression-induced flow velocity, U_b, is defined as the flow velocity at the position where 99.9% of the chemical heat is released.

The results in Figures 3 to 5 are from the same simulation of the outwardly propagating spherical stoichiometric CH_4/air flame. Figure 3 shows the normalised compression-induced flow velocity of the burned gas behind the flame front, aU_b/S_L^0, as functions of normalised flame radius and relative pressure increase. The results from the theoretical relations given by Equations (5) and (6) agree well with those from simulation. Note that to the zeroth order of accuracy, we have $S_u \approx S_L^0$ (S_u is the stretched flame speed while S_L^0 is the planar unstretched flame speed). Therefore, according to Equations (2) and (3), aU_b/S_L^0 is approximately the relative error in evaluating the stretched flame speed, S_u, caused by neglecting the compression-induced flow, U_b. The results indicate that for normalised flame radius R_f/R_0 larger than 0.4, the error will be greater than 5%. Thus, for large flames, in order to derive accurate flame speed from experimental measurements, the flow compression effect must be considered. As will be shown in Figure 5, this error is further amplified during the linear extrapolation process to obtain the unstretched flame speed. Note that when the normalised flame radius R_f/R_0 is less than 0.5, the relative pressure increase is below 18% and the increase of the temperature of unburned mixture is less than 12 K. The

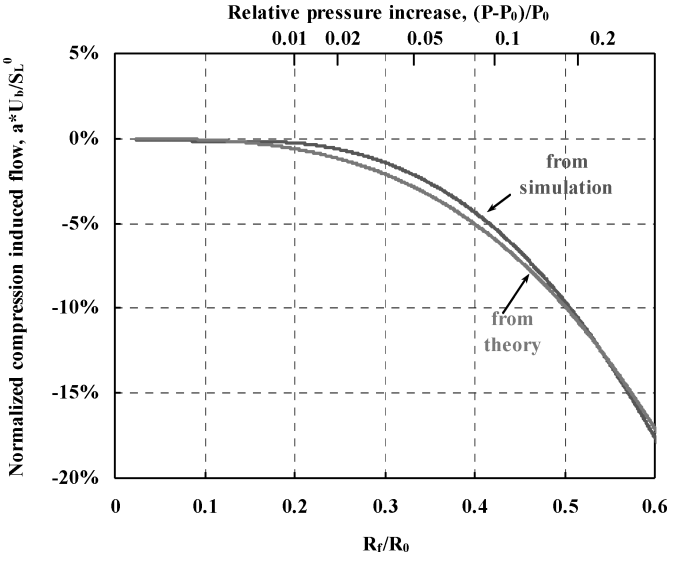

Figure 3. The compression induced flow velocity during the propagation of a spherical stoichiometric CH_4/air flame ($R_0 = 6$ cm).

resulting change of the laminar flame speed is less than 1%, which is negligible compared to the change caused by compression-induced flow.

The flow compression effect on the stretched flame speed is further demonstrated in Figure 4, in which different methods are employed to calculate the stretched flame speed, S_u. The normalised stretch rate is defined as $K' = K\delta/S_L^0$, with $\delta = 0.2$ mm and $S_L =$

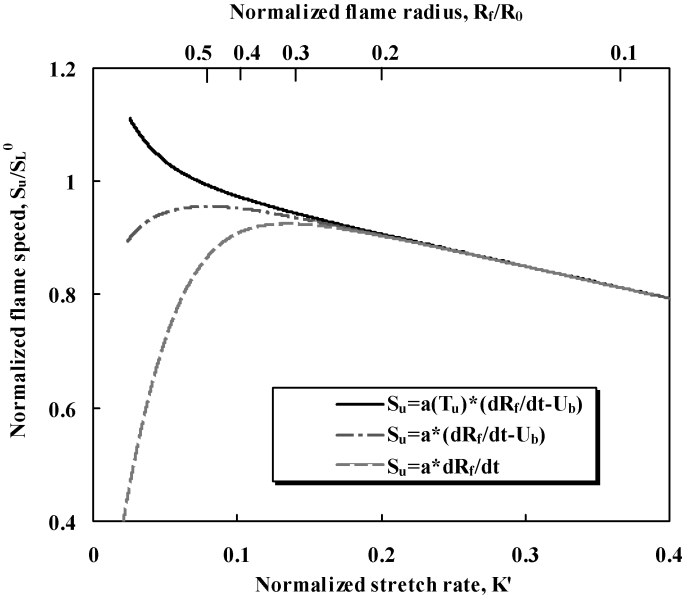

Figure 4. Normalised stretched flame speed as a function of normalised stretch rate and flame radius for a stoichiometric CH_4/air flame.

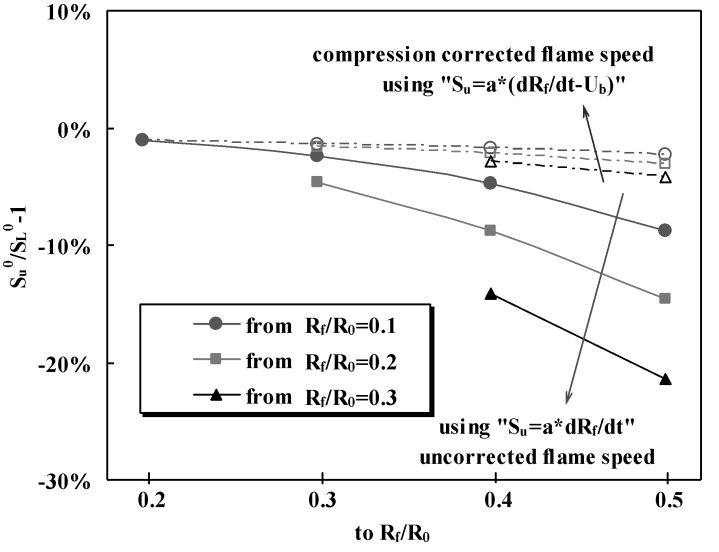

Figure 5. Accuracy of the unstretched flame speed with and without compression correction using different flame radius ranges for a stoichiometric CH_4/air flame.

37.2 cm/s being the unstretched adiabatic laminar planar flame thickness and flame speed, respectively. Figure 4 reveals that if the effect of flow compression is not considered, i.e. $S_u = a(dR_f/dt)$, S_u decreases with the increase of flame size when $R_f/R_0 > 0.3$. This is due to the fact the flame front propagating speed is decreased by the compression-induced flow (note that U_b is negative as shown in Figure 3). This result is similar to the experimental results shown in Figure 1. The rapid decrease of flame speed at large flame radii (or small stretch rate) renders the linear extrapolation to zero stretch rate inaccurate. Therefore, in order to obtain an accurate unstretched flame speed (S_u^0) from the linear extrapolation of $S_u - K$ according to Equation (1), the upper bound, R_{fU}, must be chosen to make $R_{fU}/R_0 < 0.3$ such that the effect of the compression-induced flow is prevented. Otherwise, the flame speed will be under-predicted. For a small combustion chamber of $R_0 = 6$ cm, the R_{fU} that satisfies $R_{fU}/R_0 < 0.3$ is 1.8 cm. As such, the flame radii range, $[R_{fL}, R_{fU}]$, for which the constant pressure relations are accurate, is [0.6 cm, 1.8 cm] (usually R_f is chosen to be $R_f > 0.6$ cm to prevent spark ignition effects [34]). This flame radius range might be too narrow for accurate linear extrapolation. Therefore, the compression-induced flow velocity, U_b, could be considered to extend the upper bound, R_{fU}. Figure 4 shows that when the flow velocity, U_b, is considered, i.e. $S_u = a(dR_f/dt - U_b)$, without including the temperature change, S_u will monotonically increase during flame propagation (increase of R_f) until $R_f/R_0 > 0.52$. Therefore the upper bound, R_{fU}, is extended more than 70% by considering the compression-induced flow velocity, U_b. The decrease of S_u for $R_f/R_0 > 0.52$ is caused by the change of density ratio, a, with the increase of the unburned gas temperature, T_u, as mentioned previously, and thus the density ratio is a function of T_u instead of being constant, i.e. $a = a(T_u)$, which is given by Equation (7). Accordingly, Figure 4 shows that if the change of density ratio is also considered, i.e. $S_u = a(T_u)\cdot(dR_f/dt - U_b)$, S_u monotonically increases during the whole flame propagation process as is expected for a positive Markstein length mixture and a flame with increasing T_u. It should be noted that when the pressure increase is small ($(P - P_0)/P_0 < 2\%$ or $R_f/R_0 < 0.25$), the compression

inducted flow, U_b, is negligible and thus the stretched flame speeds calculated from all three methods are nearly the same. However, the two CCFS methods yield linear relationships with stretch rate, as predicted by theory, for larger spans of data.

To reveal how the choice of flame radius range affects the measured laminar flame speed by the flow compression effect, the accuracy of the unstretched flame speed with and without the flow compression correction using different flame radii ranges $[R_{fL}, R_{fU}]$ are shown in Figure 5. The unstretched flame speed, S_u^0, is extrapolated from the plot of $S_u - K$ according to Equation (1) and $S_L^0 = 37.2$ cm/s is the planar unstretched laminar flame speed at the room temperature and pressure obtained from the 1-D planar flame simulation. When the compression effect is neglected, i.e. $S_u = a(dR_f/dt)$, Figure 5 shows that the flame radius range affects greatly the extrapolated unstretched flame speed, S_u^0: with the increase of the upper bound of the flame radius, S_u^0, is significantly under-predicted (by more than 20%). This large discrepancy reveals that the flow compression effect on flame speed is magnified by the linear extrapolation to zero stretch rate. However, when the compressed induced flow velocity, U_b, is considered and the CCFS is employed, i.e. $S_u = a(dR_f/dt - U_b)$, the discrepancies between the extrapolated unstretched flame speed, S_u^0, using different flame radii ranges are all below 5%. Therefore, a significant improvement in the accuracy of flame speed measurements is achieved using the CCFS, which considers the compression-induced flow. A typical data range utilised in previous experiments is [1.0 cm, 2.5 cm]. For chambers of radius larger than 10 cm ($R_0 = 30$ cm in [8] and [9], 13 cm in [11], 18 cm in [12], 19 cm in [13], 25 cm in [16]), the accuracy of flame speed measurement neglecting the compression effect is below 5% according to Figure 5. However, these experiments are for measurements below 5 atmosphere. For measurements of flame speed at high pressures (above 10 atmosphere), smaller chamber should be utilised for safety issues and only flame of small size could be used because hydrodynamic instability and/or thermal diffusive instability, making flame front wrinkled, will occur earlier at higher pressures [10]. When a chamber of 5 cm in radius is utilised, to use the data range of [1.0 cm, 2.5 cm] will result in error of 15%. Only when the CCFS is employed, the error becomes less than 5%.

Figure 6 shows the accuracy of the unstretched flame speed for stoichiometric H_2/air and C_3H_8/air flames, respectively. The results are similar to those of CH_4/air mixtures. All the results demonstrate that: 1), the compression-induced flow and flame radius range have significant impacts on the accuracy of the measured flame speed; 2), the compression-induced flow can be accurately predicted by the analytical correlation given by Equations (5) and (6); 3), the accuracy of the flame speed measurements can be greatly improved using the CCFS; and 4), for high-pressure experiments using small chambers, CCFS should be utilised to obtain accurate flame speed.

3.2. *Results for the constant volume method*

For the constant volume method, the pressure history, $P = P(t)$, from simulation is used to calculate the flame speed without stretch correction according to Equations (11) and (6). The SCFS is calculated from the pressure history using the procedure proposed in section 2.2. Before obtaining the SCFS, the validity of the theoretical relationships between flame radius and pressure given by Equation (6) and the linear relationship between the mass fraction of burned gas and pressure rise given by Equation (10) is demonstrated by their agreement with numerical simulation of propagation spherical flames in a closed spherical chamber. The results for a rich H_2/air flame at the equivalence ratio of $\varphi = 4$ are shown in Figure 7, which reveals that the theoretical model agrees well with the numerical simulation.

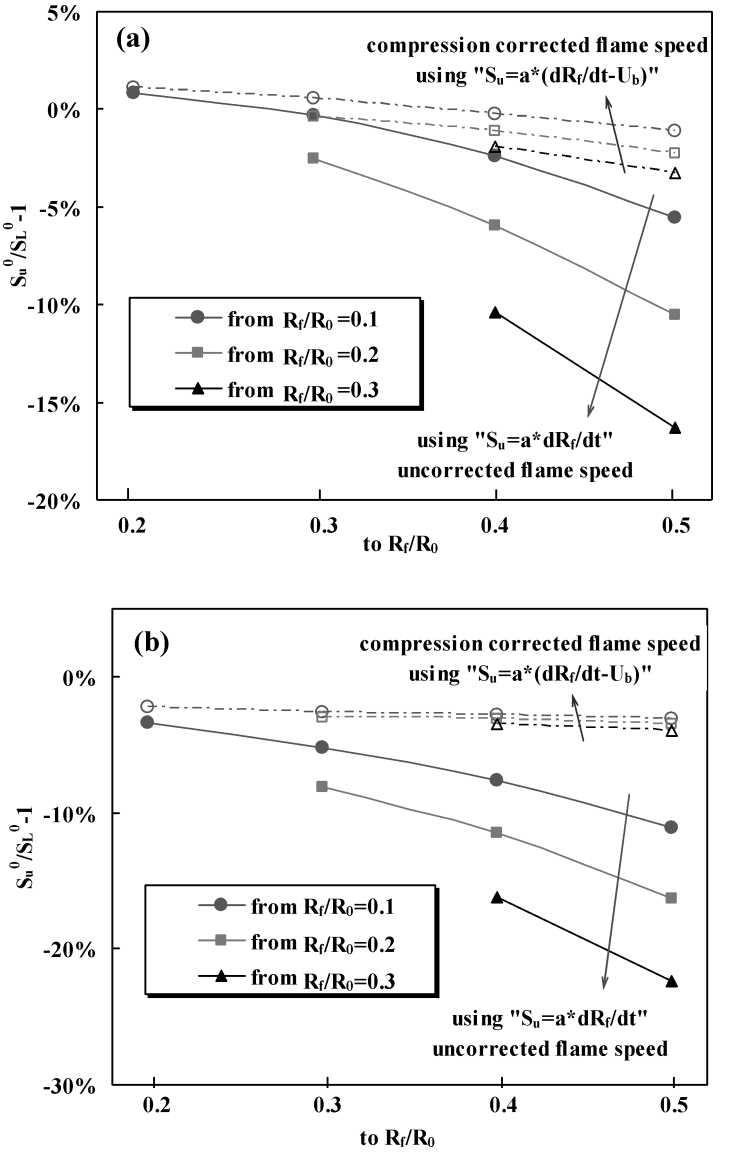

Figure 6. Accuracy of the unstretched flame speed with and without compression correction using different flame radius ranges for (a), a stoichiometric H_2/air flame; (b), a stoichiometric C_3H_8/air flame.

Similar results for other fuels are also obtained, indicating the robustness of the theoretical relationships given by Equations (6) and (10).

In order to obtain the stretch-corrected flame speed (SCFS), the Markstein length, L_u, must be extracted from the pressure history. As mentioned before, the temperature and pressure of unburned gas increase during the flame propagation. As a result, the Markstein length, L_u, which depends on pressure and temperature may also change. In the following, the Markstein length is obtained from two different methods. The first method ($L_u \neq const$) is to use $R_f = R_f(t)$ results from numerical simulation to obtain the Markstein length from

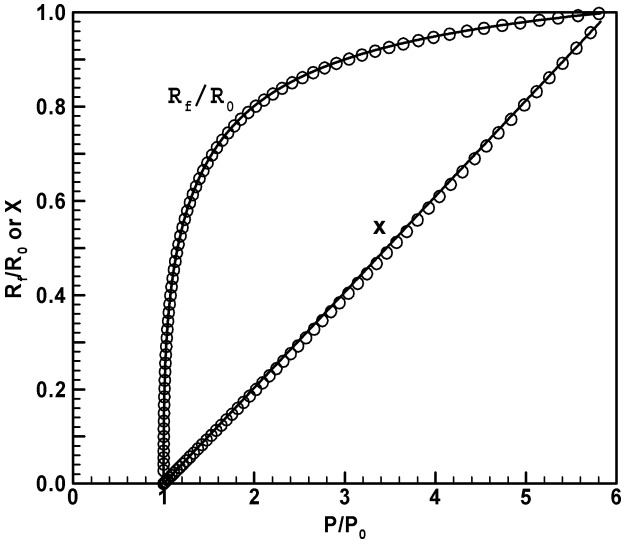

Figure 7. The change of normalised flame radius, R_f/R_0, and fraction of burned gas, x, with normalised pressure, P/P_0, during the propagation of a spherical H_2/air flame of $\varphi = 4$ in a closed spherical bomb. The lines are from theory (Equations (6) and (10) with $\gamma = 1.4$) while the symbols are from simulation.

the linear extrapolation of stretched flame speed, S_u, and stretch rate, K, at constant pressure and temperature calculated from the constant pressure method. This process is repeated to obtain the Markstein length at different temperature and pressures corresponding to those for flames at different sizes in the constant volume method. Unfortunately, in most cases, it is impossible to calculate the Markstein length accurately using the above method because a validated mechanism is usually not available and when applying the SCFS method to correct experimental data in future work, the first method of calculating the Markstein length cannot be implemented. The second method ($L_u = L_u^0 = const$) is to use the $P = P(t)$ history which could be obtained from experiments to obtain the Markstein length from linear extrapolation of S_u and K calculated from pressure history (according to Equations (11), (13) and (6)). In addition, in order to remove the effect of pressure and temperature increase, the data range used for the the Markstein length calculation is limited to those with pressure increase less than 5%. The results show that the Markstein length obtained by the second method agree well (less than 2% difference) with those obtained from the first method. The Markstein lengths obtained from the two different methods above will be used to calculate the SCFS.

The propagating spherical flames of different fuels are simulated and the results are shown in Figures 8 and 9. For a rich H_2/air flame of the equivalence ratio of $\varphi = 4$, the Markstein length corresponding to mixture at the initial pressure and temperature (1 atm, 298 K), is 0.3 mm which is predicted well by both methods. Figure 8(a) shows that without the stretch correction the flame speed from the constant volume method (using Equations (11) and (6)) agree well with those from PREMIX (PREMIX calculations are done at different sets of temperature and pressure according to the expected rise as the flame kernel grows in the constant volume vessel) only at a very large pressure increase (large R_f/R_0). When the pressure increase or the relative flame radius is small, the discrepancy between the flame speed without and with stretch correction is more than 20%. This result shows

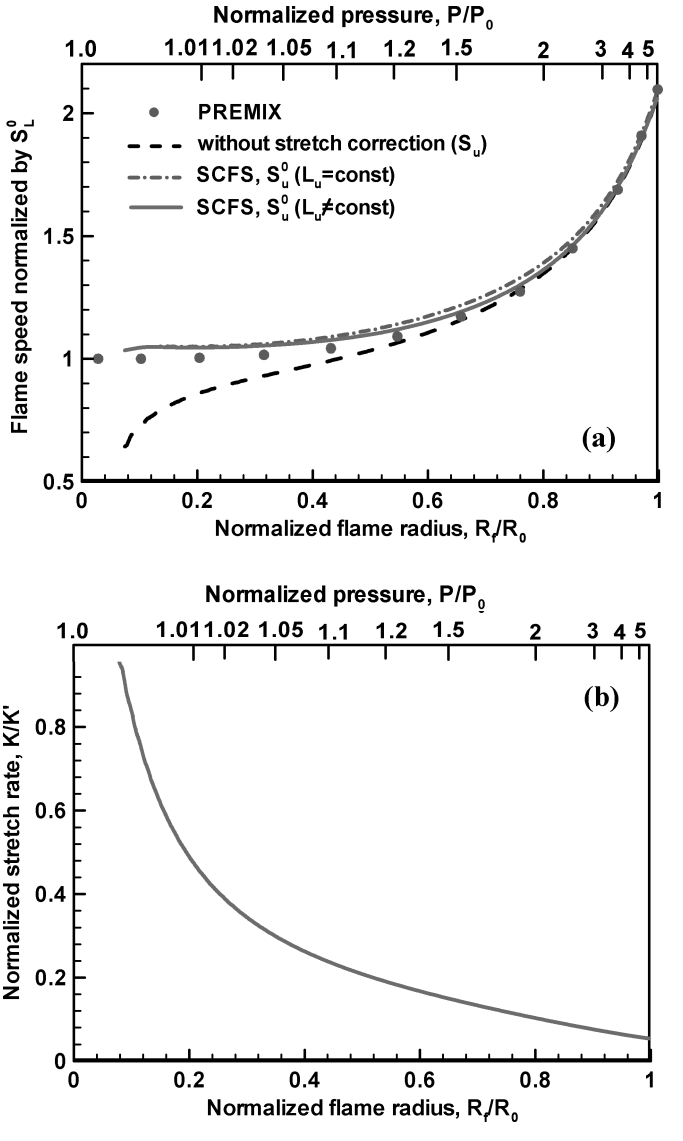

Figure 8. (a) Flame speed ($S_L^0 = 171$ cm/s) with and without stretch correction and (b) normalised stretch rate ($K' = 1850\ s^{-1}$) as a function of normalised flame radius and pressure for a H_2/air flame of $\varphi = 4$.

clearly that a stretch correction is necessary in the constant volume experiment to obtain a reliable flame speed for small spherical flames. Figure 8(a) shows that the SCFS agrees very well with those from PREMIX, even at small pressure increases. Therefore, the accuracy of the measured flame speed is greatly improved by utilising the SCFS.

The results indicate that the SCFS using the Markstein lengths from the above two methods ($L_u \neq const$ and $L_u = const$) agree very well. In fact, using a constant Markstein length from the second method only slightly over-predicts the stretch effect because the Markstein length and stretch rate decreases with the increase of pressure. As shown in

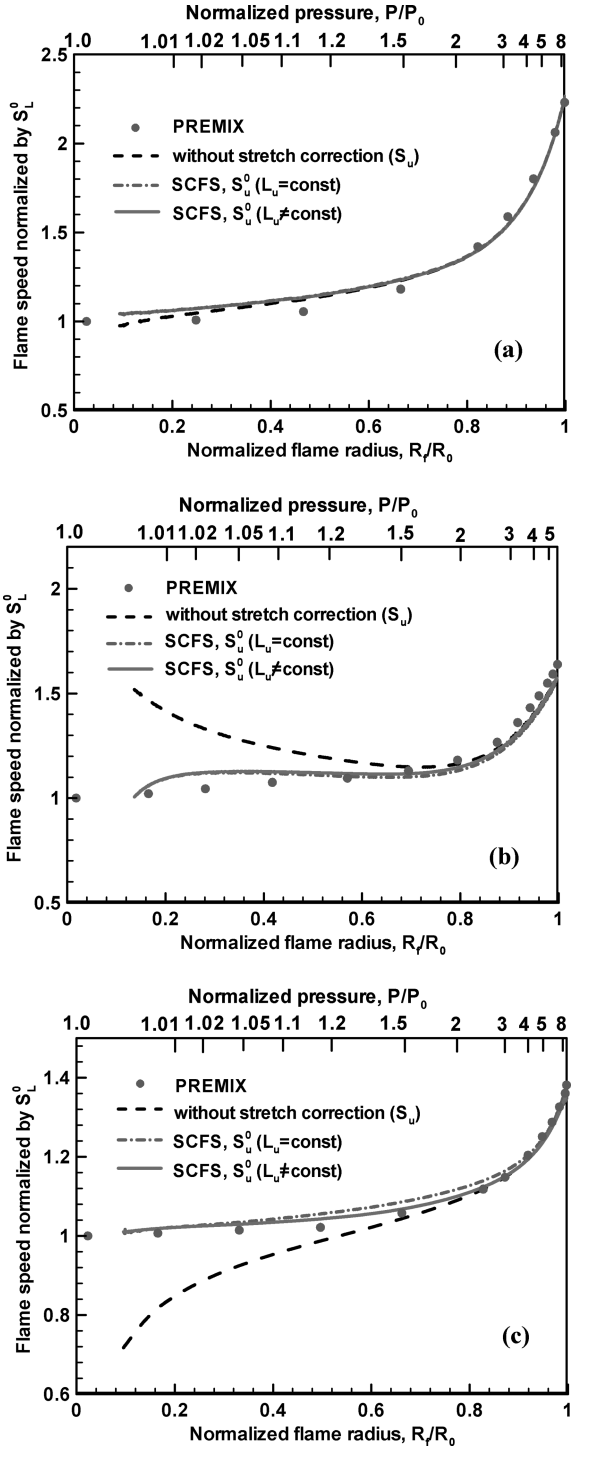

Figure 9. Flame speed with and without stretch correction as a function of normalised flame radius and pressure for (a), a H_2/air flame of $\varphi = 1$ ($S_L^0 = 206$ cm/s); (b), a H_2/air flame of $\varphi = 0.45$ ($S_L^0 = 38$ cm/s); (c), a C_3H_8/air flame of $\phi = 0.8$ ($S_L^0 = 31$ cm/s).

Figure 8(b), the stretch rate (normalised by stretch rate at $R_f/R_0 = 0.1$) quickly decreases with the increase of pressure. This explains why the difference between the SCFS obtained using the first and second methods is negligible. The success of the second method is significant for experimental measurements of flame speed by using the constant volume method: the SCFS can be obtained directly from the pressure history without any knowledge of chemical kinetics and transport properties.

For a stoichiometric H_2/air flame of $\varphi = 1$, the unburned Markstein length is 0.03 mm at the initial pressure and temperature (1 atm, 298 K). Therefore, as expected, the error caused by neglecting the stretch effect is small (below 5% for this case), which is also confirmed by results shown in Figure 9(a). It is seen that for the stoichiometric H_2/air mixture, which has a small unburned Markstein length, the stretch effect is negligible and the discrepancy between the flame speed without and with stretch correction is small.

For a lean H_2/air flame of $\varphi = 0.45$, the unburned Markstein length is negative, $L_u = -0.28$ mm at the initial pressure and temperature (1 atm, 298 K). As such, the positive flame stretch will increase the flame speed according to Equation (1). As shown in Figure 9(b), flame speed without stretch correction is much larger than the planar unstretched flame speed predicted by PREMIX. The discrepancy between the flame speed without and with stretch correction can reach as high as 50% for this case. Figure 9(c) shows that after the stretch correction, the flame speed obtained from the constant volume method agrees well with those computed from PREMIX. Therefore, the above results show that the accuracy of the flame speed measurement can be greatly improved by utilising the SCFS. Of course, in experiments for lean H_2/air flames, cellular instability will greatly affect the flame speed when the flame radius is larger than a critical value. Nevertheless, the results of lean H_2/air flame are presented here in order to demonstrate the validity of the analytical relation for the stretch effect given by Equation (14), and the improvement of the flame speed measurements accuracy by using SCFS.

For a stoichiometric CH_4/air flame, similar results to those of stoichiometric H_2/air shown in Figure 9(a) are obtained. It is found that the stretch effect is negligible since the Markstein length is small, which agrees with the prediction from Equation (14).

For a lean C_3H_8/air flame of $\varphi = 0.8$, the unburned Markstein length is 0.19 mm at the initial pressure and temperature (1 atm, 298 K). Figure 9(c) shows that when the pressure increase or the relative flame radius is small, the discrepancy between the flame speed with and without the stretch correction is more than 20%. After the stretch correction, the flame speeds from the constant volume method agree very well with those from PREMIX. Again, the accuracy of the measured flame speed is shown to be greatly improved by utilising the SCFS. All the results in Figure 9 show that the SCFS based on Markstein lengths obtained from the two methods are also in a good agreement.

Therefore, all the numerical results of H_2/air, CH_4/air and C_3H_8/air mixtures show that for mixtures of large unburned Markstein lengths, the stretch effect on flame speed measurement in the constant volume method is significant and that the SCFS should be calculated to improve the accuracy of the flame speed measurements. Without stretch correction, only the data of spherical flame with normalised radius larger than 0.6 could be utilised (Figures 8(a), 9(b) and 9(c)). After stretch correction, the SCFS agrees well with that from PREMIX and could be utilised as unstretched laminar flame speed for spherical flame with normalised radius larger than 0.1. So the present SCFS method not only greatly improves the accuracy of the flame speed measurements but also extends the parameter range of experimental conditions for which accurate measurements can be gathered. Since the proposed methods do not need information about transport and kinetic properties of the mixtures, these methods are can be directly implemented in experimental measurements.

4. Conclusions

The constant pressure and constant volume methods utilising propagating spherical flames for laminar flame speed measurements are studied theoretically and numerically. The effects of flow compression and flame stretch on the accuracy of the laminar flame speed determination are investigated and new methods to obtain more accurate flame speeds in a broader experimental range by correcting the flow compression and stretch effects are presented. The principal conclusions are:

1. For the constant pressure method, it is found that the compression induced flow can greatly affect both the instantaneous stretched and extrapolated unstretched flame speeds. When the compression effect is neglected, the choice of flame radii range significantly affects the extrapolated unstretched flame speed. Moreover, due to the flow compression effect, the maximum flame radius, below which accurate measurements can be gathered in experiment, is severely restricted. An analytical expression is derived to evaluate the compression-induced flow velocity from the flame front history. A compression-corrected flame speed (CCFS) method for flame speed measurement is proposed. Numerical simulations of hydrogen/air, methane/air, and propane/air flames using detailed chemistry demonstrate that the present CCFS method not only increase the accuracy of the measured flame speed but also extend the parameter range of experimental conditions. For high-pressure experiments in which small chambers are used, CCFS should be utilised to obtain accurate flame speed measurements.
2. For the constant volume method, an analytical expression is derived to evaluate the stretch effect on the determination of flame speed. It is found that the stretch effect is proportional to the Markstein length and inversely proportional to the flame size. For mixtures with Lewis numbers greatly deviating from unity, the stretch effect on flame speed is significant. A stretch-corrected flame speed (SCFS) model is then proposed to obtain accurate flame speed directly from the experimental measurement. The accuracy of the measured flame speed is greatly improved by using the SCFS method, which is also demonstrated by detailed numerical simulation.

The present results indicate that extrapolation of unstretched flame speeds in larger bombs at low pressures using typical flame radius ranges yield accurate results (within 5%) without consideration of the compression effects. However, in smaller bombs, they reveal that the extrapolation is subject to large errors ($\sim$15%) if these effects are not considered. Moreover, the errors become even more serious. The proposed improvements to the theoretical models not only increase the accuracy of flame speed measurements but also enable flame speed measurements to be gathered from small bombs, which has significant advantages in terms of pressure range, cost, and reduction of flame wrinkling and radiation effects, without sacrificing accuracy.

Acknowledgements

This work was partially supported by the U. S. Department of Energy (DE-FG26-06NT42716) and the Petroleum Research Fund from American Chemistry Society (PRF# 43460-AC5). The helpful comments from all the anonymous reviewers are appreciated.

References

[1] G.E. Andrews and D. Bradley, *Determination of burning velocities: a critical review*, Combust. Flame. 18 (1972), pp. 133–153.

[2] M. Metghalchi and J.C. Keck, *Laminar burning velocity of propane–air mixtures at high-temperature and pressure*, Combust. Flame. 38 (1980), pp. 143–154.

[3] C.K. Law, C.J. Sung, H.Wang and T.F. Lu, *Development of comprehensive detailed and reduced reaction mechanisms for combustion modeling*, AIAA J. 41 (2003), pp. 1629–1646.

[4] X. Qin and Y.G. Ju *Measurements of burning velocities of dimethyl ether and air premixed flames at elevated pressures*, Proc. Comb. Inst. 30 (2005), pp. 233–240.

[5] J.T. Farrell, R.J. Johnston and I.P. Androulakis, *Molecular structure effects on laminar burning velocities at elevated temperature and pressure*. SAE paper 2004–01–2936. 2004.

[6] C.J. Rallis and A.M. Garforth, *The determination of laminar burning velocity,* Prog. Energy and Combust. Sci. 6 (1980), pp. 303–329.

[7] K.T. Aung, M.I. Hassan and G.M. Faeth, *Flame stretch interactions of laminar premixed hydrogen/air flames at normal temperature and pressure*, Combust. Flame. 109 (1997), pp. 1–24.

[8] S.C. Taylor, *Burning velocity and the influence of flame stretch,* Ph.D. thesis, University of Leeds, 1991.

[9] M.J. Brown, I.C. McLean, D.B. Smith and S.C. Taylor, *Markstein lengths of CO/H_2/air flames, using expanding spherical flames*, Proc. Combust. Inst. 26 (1996), pp. 875–881.

[10] S.D. Tse, D.L. Zhu and C.K. Law, *Morphology and burning rates of expanding spherical flames in H_2/O_2/inert mixtures up to 60 atmospheres*, Proc. Combust. Inst. 28 (2000), pp. 1793–1800.

[11] S. Kwon, L.K. Tseng and G.M. Faeth, *Laminar burning velocities and transition to unstable flames in $H_2/O_2/N_2$ and $C_3H_8/O_2/N_2$ mixtures*, Combust. Flame. 90 (1992), pp. 230–246.

[12] K.T. Aung, M.I. Hassan and G.M. Faeth, *Effects of pressure and nitrogen dilution on flame/stretch interactions of laminar premixed $H_2/O_2/N_2$ flames,* Combust. Flame. 112 (1998), pp. 1–15.

[13] D. Bradley, R.A. Hicks, M. Lawes, C.G.W. Sheppard and R. Woolley, *The measurement of laminar burning velocities and Markstein numbers for iso-octane-air and iso-octane-n-heptane-air mixtures at elevated temperatures and pressures in an explosion bomb*, Combust. Flame, 115 (1998), pp. 126–144.

[14] Z. Huang, Y., Zhang, K. Zeng, B. Liu, Q. Wang and D.M. Jiang, *Measurements of laminar burning velocities for natural gas–hydrogen–air mixtures,* Combust. Flame. 146 (2006), pp. 302–311.

[15] Z. Chen, X. Qin, Y.G. Ju, Z.W. Zhao, M. Chaos and F.L. Dryer, *High temperature ignition and combustion enhancement by dimethyl ether addition to methane–air mixtures*, Proc. Combust. Inst. 31 (2007), pp. 1215–1222.

[16] F. Halter, C. Chauveau, N. Djeballi–Chaumeix and I. Gokalp, *Characterization of the effects of pressure and hydrogen concentration on laminar burning velocities of methane–hydrogen–air mixtures*, Proc. Combust. Inst. 30 (2005), pp. 201–208.

[17] B. Lewis and G. Von Elbe, *Combustion flames and explosive of gases*. 2nd ed. Academic Press, New York, 1961.

[18] D. Bradley and A. Mitcheson, *Mathematical solutions for explosions in spherical vessels*. Combust. Flame. 26 (1976), pp. 201–217.

[19] P.G. Hill and J. Hung, *Laminar burning velocities of stoichiometric mixtures of methane with propane and ethane additives,* Combust. Sci. Technol. 60 (1988), pp. 7–30.

[20] K. Saeed and C.R. Stone, *Measurements of the laminar burning velocity for mixtures of methanol and air from a constant-volume vessel using a multizone model*, Combust. Flame. 139(2004), pp. 152–166.

[21] K. Takizawa, A. Takahashi, K. Tokuhashi, S. Kondo and A. Sekiya, *Burning velocity measurement of fluorinated compounds by the spherical-vessel method*, Combust. Flame. 141 (2005), pp. 298–307.

[22] F. Parsinejad, C. Arcari and H. Metghalchi, *Flame structure and burning speed of JP–10 air mixtures,* Combust. Sci. Technol. 178 (2006), pp. 975–1000.

[23] A.S. Huzayyin, H.A. Moneib, M.S. Shehatta and A.M.A. Attia, *Laminar burning velocity and explosion index of LPG–air and propane–air mixtures*, Fuel. 87 (2008), pp. 39–57.

[24] H. Tsuji, *Counterflow diffusion flames*, Prog. Energy and Combust. Sci. 8 (1982), pp. 93–119.

[25] C.K. Wu and C.K. Law, *On the determination of laminar flame speed from stretched flames*, Proc. Combust. Inst. 20 (1985), pp. 1941–1949.
[26] F.N. Egolfopoulos, P. Cho and C.K. Law, *Laminar flame speeds of methane air mixtures under reduced and elevated pressures*, Combust. Flame. 76 (1989), pp. 375–391.
[27] Y. Huang, C.J. Sung and J.A. Eng, *Laminar flame speeds of primary reference fuels and reformer gas mixtures,* Combust. Flame. 139 (2004), pp. 239–251.
[28] A. Levy and F.J. Weinberg, *Optical flame structure studies: Some conclusions concerning the propagation of flat flames*, Proc. Combust. Inst. 7 (1959), pp. 296–303.
[29] A. Van Maaren, D.S. Thung and L.P.H. Degoey, *Measurement of flame temperature and adiabatic burning velocity of methane/air mixtures,* Combust. Sci. Technol. 96 (1994), pp. 327–344.
[30] M.P. Burke, Z. Chen, Y. Ju and F.L. Dryer, *Effect of cylindrical confinement on the determination of laminar flame speeds using outwardly propagating flames,* Combust. Flame. 2009. in press. Accepted.
[31] Z. Chen, M.P. Burke and Y. Ju, *Effect of radiation on the determination of laminar flame speed using propagating spherical flames,* SIAM 12th International Conference on Numerical Combustion. Monterey, California, USA, 2008.
[32] A.P. Kelly and C.K. Law, *Nonlinear effects in the experimental determination of laminar flame properties from stretched flames*. Fall technical meeting: Eastern states sections of the combustion institute, Virginia, Paper B–11. 2007.
[33] Z. Chen, M.P. Burke and Y. Ju, *Effects of Lewis number and ignition energy on the determination of laminar flame speed using propagating spherical flames,* Proc. Combust. Inst. 32 (2009), pp. 1253–1260.
[34] D. Bradley, P.H. Gaskell, and X.J. Gu. *Burning velocities, Markstein lengths, and flame quenching for spherical methane–air flames: a computational study*, Combust. Flame. 104 (1996), pp. 176–198.
[35] P. Clavin, *Dynamic behavior of premixed flame fronts in laminar and turbulent flows,* Prog. Energy Combust. Sci. 11 (1985), pp. 1–59.
[36] N. Peters, *Turbulent combustion,* Cambridge University Press, New York, 2000.
[37] G.I. Sivashinsky, *Propagation of a flame in a closed vessel*, Israel J. Technol. 12 (1974), pp. 317–321.
[38] G.I. Sivashinsky, *Hydrodynamic theory of flame propagation in an enclosed volume*, Acta Astronautica. 6 (1979), pp. 631–645.
[39] J.K. Bechtold and M. Matalon, *Some new results on Markstein number predictions.* AIAA–2000–0575. 2000.
[40] Z. Chen, M. Qin, B. Xu, Y.G. Ju and F.S. Liu, *Studies of radiation absorption on flame speed and flammability limit of CO_2 diluted methane flames at elevated pressures*, Proc. Combust. Inst. 31 (2007), pp. 2693–2700.
[41] G. Strang, *On construction and comparison of difference schemes*, SIAM J. Numer. Analysis. 5 (1968), pp. 506–517.
[42] B. van Leer, *On the relation between the upwind–differencing schemes of Godunov, Engquist-osher and Roe,* SIAM J. Sci. Statist. Comput. 5 (1984), pp. 1–20.
[43] P.N. Brown, G.D. Byrne and A.C. Hindmarsh,, *VODE: A variable-coefficient ODE solver,* SIAM J. Sci. Statist. Comput. 10 (1989), pp. 1038–1051.
[44] R.J. Kee, J.F. Grcar, M.D. Smooke and J.A.Miller, *A FORTRAN program for modeling steady laminar one-dimensional premixed flames*, Sandia National Laboratory Report SAND85–8240, 1985.
[45] R.J. Kee, F.M., Rupley and J.A. Miller, C*hemkin-II: A FORTRAN package for the analysis of gas-phase chemical kinetics*, Sandia National Laboratory Report SAND89-8009B, 1989.
[46] Z. Chen and Y. Ju, *Theoretical analysis of the evolution from ignition kernel to flame ball and planar flame,* Combust. Theory Modelling. 11 (2007), pp. 427–453.
[47] J. Li, Z.W. Zhao, A. Kazakov and F.L. Dryer, *An updated comprehensive kinetic model of hydrogen combustion*, Int. J. Chem. Kinetics. 36 (2004), pp. 566–575.
[48] Available online from: http://www.me.berkeley.edu/gri_mech/.
[49] Available online from: http://maeweb.ucsd.edu/∼combustion/.